Contribution from the Laboratoire de Chimie de Coordination, associé au CNRS (ERA 670), Université Louis Pasteur, 67000 Strasbourg Cedex, France, and Laboratoire de Chimie de Coordination du CNRS, 31030 Toulouse Cedex, France

Synthesis, Crystal Structure, and Electronic Properties of (L-Methionylglycinato)copper(II)

J. DEHAND,* J. JORDANOV, F. KECK, A. MOSSET, J. J. BONNET, and J. GALY

Received July 20, 1978

The crystal and molecular structure of (L-methionylglycinato)copper(II) has been determined by single-crystal X-ray diffraction. Crystal data: orthorhombic system, space group $P2_12_12_1$, cell data $a = 9.889$ (2) Å, $b = 11.548$ (1) Å, $c = 9.337$ (2) Å, $\alpha = \beta = \gamma = 90°$, $Z = 4$, $V = 1066$ Å^3, 1369 reflections. The dipeptide serves as a pentadentate ligand to three different Cu atoms with square-pyramidal geometry. The amino nitrogen atom, the ionized amide nitrogen atom, and one of the carboxylate donor atoms are equatorially disposed about one Cu atom, while the free carboxyl oxygen atom bridges to a neighboring copper atom. The peptide oxygen occupies the apical position of yet another Cu atom; the bond angle value of Cu–O(1)–C(2) (152.6°) is unusually high. No hydrogen bonding is observed as intermolecular interaction. The spectroscopic properties, as compared with those of the parent (glycyl-L-tyrosinato)(diaquo)copper(II) dihydrate, show that complex formation starts probably in aqueous solution with the terminal amino group. UV–visible absorption spectra results suggest that the structure found in the crystal does not persist in aqueous solution or in KBr pellets. A cleavage of the carboxylate bridge occurs and one of the carboxyl oxygen atoms is progressively replaced, either by a bromide or by a water molecule.

The binding of metal ions to peptides has been a subject of increasing interest over the past 2 decades,[1-4] largely because many of these reactions provide simple models for the much more complex enzymes such as endo- and exopeptidases.[5] The latter are zinc metallo enzymes, and replacement of the active site Zn(II) ion with Cu(II), which displays more interesting spectroscopic properties,[6] has been known to result in a complete loss of the enzyme catalytic activity.[7,8] Recently, however, Schneider et al.[9] reported that copper(II) carboxypeptidase A shows a substantial degree of activity in the hydrolysis of L-*S*-(*trans*-cinnamoyl)-α-mercapto-β-phenylpropionate.

The peptide bond

$$-\overset{\overset{O}{\|}}{C}-NH-$$

is a difficult bond to break. It has been suggested by Ludwig and Lipscomb,[10] on the basis of carboxypeptidase A structural studies, that the metal ion polarizes the C=O bond, increasing the electrophilic character of the carbonyl carbon so that it is more readily attacked, either by water or by a nucleophile on the proteins. Freeman has extensively reviewed[11] the main types of potentially metal-binding atoms in various di- and tripeptides. At low pH values (<4), the peptide group binds weakly through its oxygen. In the pH range 4–7, coordination occurs preferentially through the deprotonated amide nitrogen.

Recently, the X-ray structures of (glycyl-L-methioninato)copper(II)[12] [Cu(GM)] and (glycyl-L-alaninato)copper(II) hydrate [Cu(gly-L-ala)][13] have been reported. They are, to our knowledge, the two first examples of axial coordination of copper by an oxygen peptide atom. Although in the (GM)Cu^{II} crystal structure the thioether of the side chain of the amino acid residue is not involved in any metal interaction, it was of interest to confirm if it can participate in the complex formation. Indeed, donor atoms present in the side chains of amino acid residues can participate in complex formation. In this regard thioether groups, although generally considered to have little affinity with "class a" metal ions such as Cu(II),[11,14] have recently been claimed to represent the ligating S-donor atom(s) in blue copper proteins.[15-19]

In the framework of a systematic study of copper(II) dipeptide systems[20,21] we report here the synthesis and crystallographic investigation of Cu(MG) (where MG = L-methionylglycine). An effort is made to compare the spectroscopic and electronic properties of this complex and of $[Cu(GT)(H_2O)_2]\cdot 2H_2O$[20,21] (where GT = glycyl-L-tyrosine) in order to deduce whether these structures can be predicted from the spectroscopic data and if they persist in aqueous solution.

Experimental Section

Cu(MG) was prepared by shaking an aqueous solution of MG (0.206 g, 1 mmol) with an excess of freshly precipitated copper(II) hydroxide at pH 6.5. The residual copper(II) hydroxide was removed by filtration. The volume of the solution was reduced and ethanol–diethyl ether (1:1) added. The complex crystallized out as dark blue needles, which were recrystallized from water, washed with alcohol, and air-dried. Anal. Calcd for $C_7H_{12}N_3O_3SCu$: C, 31.36; H, 4.48; N, 10.45. Found: C, 31.3; H, 4.6; N, 10.4. $[Cu(GT)(H_2O)_2]\cdot 2H_2O$ was prepared according to a published method.[20]

IR, Raman, and ^{1}H NMR Spectra Studies. The IR spectra (4000–400 cm^{-1}) were obtained from KBr pellets on a Beckman IR 12 spectrophotometer; far-IR spectra were obtained from polyethylene plates on a Polytec FIR 30 spectrometer. Raman spectra were recorded by employing powder samples for the ligand and crystals for the complexes, by using a PH1 CODERG Raman spectrometer equipped with a Coherent Radiation argon ion laser operating at 5145 Å.

^{1}H NMR spectra were recorded at room temperature on a FT Bruker WH 90 spectrometer from D_2O solution with TMPS as internal standard. For the line broadening studies, $CuCl_2$ was added as small aliquots of concentrated $CuCl_2/D_2O$ solutions to the ligand/D_2O solutions.

UV–Visible Spectra. Electronic spectra were recorded on a Beckman Acta III spectrophotometer. Solution measurements were made on water solutions (3 mmol) of the complexes in quartz cells of either 1- or 0.1-cm path lengths. Solid-state spectra were obtained from KBr pellets (3% in 0.3 g dried KBr), similar to those used in IR spectroscopy, contained between quartz plates. The combination of the quartz plates and KBr pellets was spectrally transparent over the 200–800-nm range, with only a weak rise of the baseline below 250 nm. The KBr support proved to be the best of those essayed. In mineral oil mulls the spectra are the same but not as well resolved.

Magnetic and ESR Measurements. Room-temperature magnetic moments were determined by the Gouy method using mercury(tetrathiocyanato)cobaltate(II) as a calibrant. Single-crystal and solution (1 mmol in 10% methanol/water) ESR spectra were recorded at room temperature on a Bruker ER 420 spectrometer operating at X-band frequency.

X-ray Study. Examination of crystals of copper L-methionylglycine by means of precession camera using Mo Kα radiation showed that the compound belongs to the orthorhombic system. Systematic absences $h = 2n + 1$ for $h00$, $k = 2n + 1$ for $0k0$, and $l = 2n + 1$ for 001 reflections led to the assignment of $P2_12_12_1$ (D_2^4) as the space group. Cell constants and corresponding standard deviations listed in Table I were derived after least-squares refinement of the settings of 25 reflections automatically centered on a CAD4 Enraf-Nonius

* To whom correspondence should be addressed at the Université Louis Pasteur.

0020-1669/79/1318-1543$01.00/0

Table I. Experimental Details of the X-ray Diffraction Study of (L-Methionylglycinato)copper(II)

1. Physical and Crystallographic Data

crystal system: orthorhombic	absn factor: $\mu(\lambda$ Mo) = 22.9 cm^{-1}
a = 9.889 (2) Å	morphology: trigonal prism
b = 11.545 (1) Å	elongated along [001]
c = 9.337 (2) Å	mol wt 267.79
α = 90°	space group $P2_12_12_1$
β = 90°	V = 1066 Å^3
γ = 90°	Z = 4
ρ_{exptl} = 1.64 (2) g cm^{-3}	$F(000)$ = 137
ρ_X = 1.66 g cm^{-3}	

2. Data Collection

temp: 21.8 °C
radiation: molybdenum $\lambda(K\bar{\alpha})$ 0.710 69 Å
monochromatization: oriented graphite crystal
crystal-detector dist: 208 mm
detector window: height[a] = 4 mm, width[a] = 3.00 + 0.75 tan θ
takeoff angle:[a] 3.7°
scan mode: θ–2θ
max Bragg angle: 35°
scan angle: $\Delta\theta = \Delta\theta_0 + B \tan\theta$, $\Delta\theta_0$[a] = 1.1°, B[a] = 0.347°
values determining the scan speed: SIGPRE[a] = 0.33, SIGMA[a] = 0.008, VPRE[a] = 20°/min in θ, TMAX[a] = 90 s
controls: intensity, orientation
reflections: 400, 00$\bar{4}$, 040
periodicity: 7200 s

3. Conditions for Refinement

reflections for the refinement of the cell dimensions: 25
recorded reflections: 2728
independent reflections: 2668
utilized reflections: 1369 with $I > 3\sigma(I)$
refined parameters: 128
reliability factors: $R = \Sigma|k|F_o| - |F_c||/\Sigma k|F_o|$, $R_w = [\Sigma w^2(k|F_o| - |F_c|)^2/\Sigma w^2 k^2 F_o^2]^{1/2}$

[a] All these values were defined in a previous paper.[22]

computer-controlled diffractometer.

The crystal selected for data collection was a trigonal prism with bonding faces of the forms {100}, {010}, {110}, and {001}. The dimensions of the crystal are 0.15, 0.18, 0.23, and 0.57 mm. The crystal was mounted with 001 approximately along the spindle axis. Data were collected at 22 °C by θ–2θ scan method using graphite Mo Kα monochromatized radiation and following the scheme which appears in Table I and is fully described elsewhere.[22]

The data were processed in our normal way[22] using a value of p = 0.02.

Structure Determination. The structure was solved by standard Patterson and Fourier methods and refined by full-matrix least-squares techniques (in addition to local programs for the CII Iris 80, local modifications of the following programs were employed: Zalkin's Fourier program, Ibers and Doeden's NUCLS program, Busing, Martin, and Lewy's[23] ORFFE program, and Johnson's[24] ORTEP program). The quantity minimized was $\sum w([F_o] - [F_c])^2$, where $[F_o]$ and $[F_c]$ are the observed and calculated structure amplitudes and where the weights w are taken as $4F_o^2/\sigma(F_o^2)$. The agreement indices are defined in Table I. Values of the atomic scattering factors and the anomalous terms for the copper atom were taken from the Cromer and Waber tables.[25]

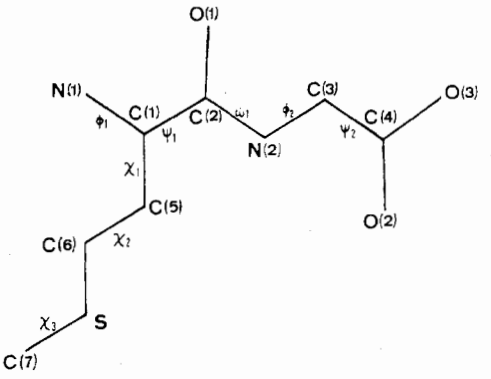

Figure 1. Torsion angles.

From the Patterson function, the Cu and S atoms were located and on a subsequent Fourier map all the atoms of the L-methionylglycine ligand were found. R and R_w were 0.104 and 0.105 after two cycles of least-squares refinements of the atomic parameters for all atoms located involving isotropic thermal parameters. The anisotropic thermal parameters were then used for all atoms and finally the secondary extinction coefficient was allowed to vary[26] ($g = 0.12 \times 10^{-6}$).

At this point, R and R_w were equal to 0.034 and 0.048, respectively. Then, a difference Fourier map clearly revealed all hydrogen atoms: their atomic position parameters with isotropic thermal parameters were allowed to vary in a final cycle of least-squares refinement which converged to the R and R_w values of 0.024 and 0.027.

In Table II, we present the atomic parameters together with their standard deviations as derived from the inverse matrix. Table III lists the main interatomic distances and angles with their standard deviation. The root-mean-square amplitudes of vibration for those atoms refined anisotropically appear in Table IV.

Results and Discussion

Description of the Molecular and Crystal Structure of the (L-Methionylglycinato)copper(II) Complex. A schematic drawing of the free dipeptide is shown in Figure 1, specifying the conformational angles and the atom numbering used. Each

Table II. Atomic Coordinates and Thermal Parameters

	x	y	z	β_{11}	β_{22}	β_{33}	β_{12}	β_{13}	β_{23}
Cu	0.28047 (5)	0.09164 (4)	0.03104 (5)	0.00467 (4)	0.00531 (3)	0.00328 (4)	−0.00126 (4)	0.00037 (4)	−0.00042 (4)
S	0.7398 (1)	0.1356 (1)	0.5043 (1)	0.0090 (1)	0.0109 (1)	0.0085 (1)	−0.0003 (1)	−0.0042 (1)	0.0006 (1)
O(1)	0.6121 (3)	0.2807 (3)	−0.0422 (3)	0.0083 (3)	0.0084 (3)	0.0056 (3)	−0.0050 (3)	0.0006 (3)	−0.0002 (3)
O(2)	0.2509 (3)	0.0259 (2)	−0.1655 (3)	0.0073 (4)	0.0072 (3)	0.0043 (3)	−0.0036 (2)	0.0016 (2)	−0.0019 (2)
O(3)	0.3330 (3)	0.0302 (2)	−0.3878 (3)	0.0069 (3)	0.0061 (3)	0.0035 (3)	−0.0020 (2)	0.0005 (3)	−0.0013 (2)
N(1)	0.3530 (3)	0.1773 (3)	0.2046 (3)	0.0055 (4)	0.0051 (3)	0.0038 (3)	−0.0008 (3)	0.0003 (3)	−0.0002 (3)
N(2)	0.4255 (3)	0.1676 (3)	−0.0610 (3)	0.0055 (3)	0.0063 (3)	0.0033 (3)	−0.0024 (3)	0.0009 (3)	−0.0005 (3)
C(1)	0.4834 (4)	0.2360 (3)	0.1724 (4)	0.0055 (4)	0.0041 (3)	0.0043 (4)	−0.0006 (3)	−0.0003 (3)	−0.0003 (3)
C(2)	0.5111 (3)	0.2306 (3)	0.0086 (4)	0.0051 (4)	0.0040 (3)	0.0041 (4)	−0.0004 (3)	0.0001 (3)	0.0001 (3)
C(3)	0.4411 (4)	0.1479 (4)	−0.2138 (4)	0.0070 (5)	0.0073 (4)	0.0038 (4)	−0.0024 (4)	0.0010 (4)	−0.0015 (4)
C(4)	0.3340 (4)	0.0613 (3)	−0.2586 (4)	0.0049 (4)	0.0047 (4)	0.0046 (4)	−0.0002 (3)	−0.0002 (3)	−0.0005 (3)
C(5)	0.6003 (4)	0.1792 (4)	0.2517 (4)	0.0056 (4)	0.0072 (4)	0.0048 (4)	0.0005 (4)	−0.0004 (4)	−0.0004 (4)
C(6)	0.6010 (4)	0.2040 (4)	0.4135 (4)	0.0082 (5)	0.0079 (4)	0.0053 (4)	0.0002 (4)	−0.0018 (4)	−0.0001 (4)
C(7)	0.6893 (5)	−0.0093 (5)	0.4880 (7)	0.0217 (10)	0.0074 (5)	0.0193 (11)	0.0021 (6)	−0.0097 (9)	0.0025 (6)

	x	y	z	B, Å^2		x	y	z	B, Å^2
H(N1)	0.357 (5)	0.131 (4)	0.276 (5)	1.99	H′(C5)	0.598 (5)	0.091 (4)	0.236 (5)	2.18
H′(N1)	0.302 (5)	0.234 (4)	0.220 (5)	1.99	H(C6)	0.527 (5)	0.178 (4)	0.455 (5)	2.60
H(C1)	0.479 (5)	0.320 (4)	0.186 (5)	1.74	H′(C6)	0.613 (5)	0.282 (4)	0.435 (5)	2.60
H(C3)	0.518 (5)	0.112 (4)	−0.230 (5)	2.53	H(C7)	0.74	−0.065	0.525	5.33
H′(C3)	0.423 (6)	0.217 (4)	−0.270 (5)	2.53	H′(C7)	0.70	−0.035	0.38	5.33
H(C5)	0.685 (5)	0.206 (4)	0.222 (5)	2.18	H″(C7)	0.60	−0.025	0.525	5.33

Table III. Bond Distances (Å) and Bond Angles (deg)

Cu-O(1)^{v}	2.226 (13)	C(6)-S	1.796 (13)
Cu-O(2)	2.007 (10)	S-C(7)	1.753 (8)
Cu-O(3)^{ii}	1.952 (13)	N(1)-H(N1)	0.86 (6)
Cu-N(1)	2.030 (14)	N(1)-H′(N1)	0.84 (6)
Cu-N(2)	1.888 (13)	C(1)-H(C1)	0.98 (4)
N(1)-C(1)	1.487 (9)	C(3)-H(C3)	0.88 (6)
C(1)-C(2)	1.555 (6)	C(3)-H′(C3)	0.97 (7)
C(1)-C(5)	1.522 (12)	C(5)-H(C5)	0.93 (6)
C(2)-O(1)	1.248 (9)	C(5)-H′(C5)	1.03 (5)
C(2)-N(2)	1.292 (10)	C(6)-H(C6)	0.88 (7)
N(2)-C(3)	1.453 (6)	C(6)-H′(C6)	0.93 (5)
C(3)-C(4)	1.516 (11)	C(7)-H(C7)	0.88 (8)
C(4)-O(2)	1.264 (10)	C(7)-H′(C7)	1.06 (8)
C(4)-O(3)	1.259 (6)	C(7)-H″(C7)	0.96 (8)
C(5)-C(6)	1.537 (6)		

O(1)^{v}-Cu-O(2)	100.6 (7)	N(1)-C(1)-C(2)	111.3 (5)
O(1)^{v}-Cu-O(3)^{ii}	91.6 (3)	N(1)-C(1)-C(5)	109.5 (8)
O(1)^{v}-Cu-N(1)	84.5 (6)	C(2)-C(1)-C(5)	109.1 (7)
O(1)^{v}-Cu-N(2)	106.4 (4)	C(1)-C(2)-O(1)	119.8 (7)
O(2)-Cu-O(3)^{ii}	89.9 (6)	C(1)-C(2)-N(2)	113.7 (7)
O(2)-Cu-N(2)	82.5 (6)	N(2)-C(2)-O(1)	126.4 (5)
O(3)^{ii}-Cu-N(1)	104.1 (5)	C(2)-N(2)-C(3)	120.8 (7)
N(1)-Cu-N(2)	82.4 (5)	N(2)-C(3)-C(4)	107.4 (8)
Cu-N(1)-C(1)	111.5 (6)	C(3)-C(4)-O(2)	118.6 (5)
Cu-N(2)-C(2)	122.0 (4)	C(3)-C(4)-O(3)	117.3 (7)
Cu-N(2)-C(3)	117.1 (7)	O(2)-C(4)-O(3)	124.1 (6)
Cu-O(2)-C(4)	114.3 (5)	C(1)-C(5)-C(6)	113.6 (7)
Cu-O(1)^{v}-C(2)^{v}	152.6 (3)	C(5)-C(6)-S	112.7 (7)
Cu-O(3)^{ii}-C(4)	125.6 (6)	C(6)-S-C(7)	99.2 (6)

Table IV. Root-Mean-Square Amplitudes of Vibrational Ellipsoid Axes

Cu	0.1188 (8)	0.1411 (10)	0.1987 (11)
S	0.145 (2)	0.246 (2)	0.273 (2)
O(1)	0.135 (5)	0.159 (5)	0.281 (4)
O(2)	0.125 (5)	0.144 (5)	0.260 (4)
O(3)	0.117 (5)	0.160 (5)	0.227 (4)
N(1)	0.128 (6)	0.158 (5)	0.193 (5)
N(2)	0.114 (7)	0.142 (6)	0.227 (5)
C(1)	0.134 (7)	0.158 (7)	0.176 (7)
C(2)	0.135 (7)	0.154 (7)	0.170 (6)
C(3)	0.122 (7)	0.162 (7)	0.245 (7)
C(4)	0.140 (7)	0.157 (6)	0.181 (7)
C(5)	0.144 (7)	0.166 (6)	0.222 (6)
C(6)	0.141 (7)	0.211 (7)	0.231 (7)
C(7)	0.177 (9)	0.262 (9)	0.378 (9)

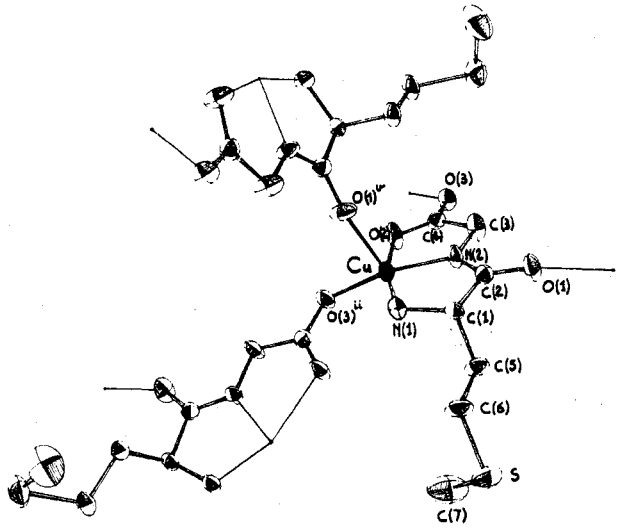

Figure 2. Coordination geometry about the copper atom.

L-methionylglycine binds (Figure 2) to one copper atom at its amino and peptide nitrogen atoms and at the carbonyl oxygen O(2) atom and to a second copper at the carboxyl O(3) atom, while a third copper atom is attached to the peptide oxygen atom. The Cu atom coordination geometry is square pyramidal, the first four donor atoms forming the N_2O_2 basis of the pyramid, while the peptide oxygen atom occupies the apical position. The O(2)–Cu–N(2) and N(1)–Cu–N(2) angles are pinched (82.5 and 82.4°, respectively) owing to the tridentate coordination, whereas the pyramid axis along Cu–O(1) is bent toward N(1). The copper atom is displaced by 0.182 Å from the basal plane (Table V). A distortion of 25% from the ideal square pyramid has been calculated,[27] comparable to the distortion observed in the copper(II) glycyl-L-tyrosine complex.[21] The methionyl side chain $-CH_2CH_2SCH_3$ and the peptide oxygen O(1) are situated trans to the pyramidal base plane. The sulfur atom does not participate, however, in the copper coordination, the nearest metal ion being respectively at 5.28, 5.78 and 5.92 Å.

Table V. Atom Distances from Least-Squares Plane

	A	B	C	D
plane 1: N(1), N(2), O(2), O(3)	−0.7236	0.6758	−0.1402	1.5145
plane 2: N(1), C(1) C(2), N(2)	−0.5372	0.8250	−0.1754	0.5564
plane 3: N(2), C(3), C(4), O(2)	−0.6169	0.7613	−0.1997	1.0030

Δ(1), Å		Δ(2), Å		Δ(3), Å	
N(1)	0.104	N(1)	0.035	N(2)	−0.006
N(2)	−0.143	C(1)	−0.046	C(3)	0.011
O(2)	0.138	C(2)	0.024	C(4)	−0.013
O(3)	−0.063	N(2)	−0.008	O(2)	0.009
Cu	0.182				

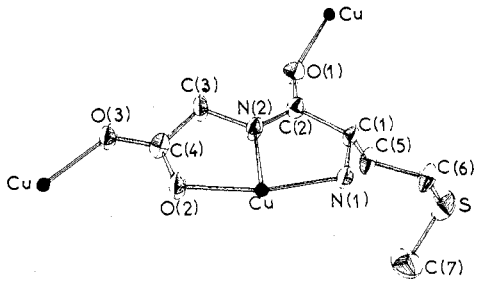

Figure 3. Ligand geometry after complexation.

Further conformational features of the dipeptide ligand in the complex (Figure 3) are as follows. The two five-membered chelate rings formed by the N(1), N(2), and O(2) tricoordination to a same metal atom are almost planar. The N(1)–C(1)–C(2)–N(2) cycle is slightly distorted from the basal plane by 0.035 Å for N(1) and −0.046 Å for C(1). This distortion is probably due to the strain resulting from the peptide oxygen O(1) binding to a second copper atom.

The peptide backbone conformation is generally determined by its conformational angles as defined by Edsall et al.[28] and listed in Table VI. The values observed for ψ_1^1 and ψ_2^1, +7° and −3°, respectively, confirm the distortion of the chelate rings and particularly of the N(1)–C(1)–C(2)–N(2) torsion angle.

The dipeptide tricoordination to the Cu atoms through the amino NH_2, the peptide N, and the carboxyl O atoms has been frequently observed,[21,29–32] although the Cu–NH_2 bond (1.888 Å) is the shortest reported to date. The carboxylate bridging interaction with two Cu atoms is of the following syn–anti type:

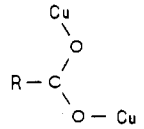

Such a configuration has already been reported by Freeman[33] for Cu and Zn complexes of aspartic and glutamic acids and by Amirthalingam[32] for (L-valyl-L-tyrosine)copper tetrahydrate. Nevertheless, the same bond order for the two

Table VI. Torsion Angles (deg)

ϕ_1^1	Cu-N(1)-C(1)-C(2)	−9
ϕ_1^2	Cu-N(1)-C(1)-C(5)	111
ϕ_2	C(2)-N(2)-C(3)-C(4)	−174
ψ_1^1	N(1)-C(1)-C(2)-N(2)	7
ψ_1^2	N(1)-C(1)-C(2)-O(1)	−176
ψ_2^1	N(2)-C(3)-C(4)-O(2)	−3
ψ_2^2	N(2)-C(3)-C(4)-O(3)	178
ω_1	C(1)-C(2)-N(2)-C(3)	176
χ_1	N(1)-C(1)-C(5)-C(6)	73
χ_2	C(1)-C(5)-C(6)-S	180
χ_3	C(5)-C(6)-S-C(7)	69

Table VII. Geometrical Differences between Cu(Gly-L-Ala), Cu(GM), and Cu(MG)

	Cu(Gly-L-Ala)[13]	Cu(GM)[12]	Cu(MG)
N(2)-C(2), Å	1.33 (1)	1.323 (6)	1.292 (10)
Cu-N(2)-C(2), deg	118.7 (8)	119.2 (3)	122.0 (4)
Cu-N(2)-C(3), deg	117.5 (8)	117.3 (2)	117.1 (7)
S-C(7), Å		1.823 (6)	1.796 (13)
S-C(7), Å		1.800 (7)	1.753 (8)

Table VIII. Shortest Intermolecular Distances (Å) within the Cell Unit[a]

N(1)-O(2)^{ii}	2.83	O(3)^{ii}-O(1)^{v}	3.00
N(1)-O(3)^{ii}	3.14	O(2)-O(3)^{ii}	2.80
N(1)-O(1)^{v}	2.86	N(1)-S^{vi}	3.65
O(2)-O(1)^{v}	3.26		

[a] (i) x, y, z; (ii) $1/2 - x, \bar{y}, 1/2 + z$; (iii) $1/2 + x, 1/2 - y, z$; (iv) $\bar{x}, 1/2 + y, 1/2 - z$; (v) $x - 1/2, 1/2 - y, \bar{z}$; (vi) $x - 1/2, 1/2 - y, 1 - z$.

C–O of the carboxylic group have been observed only in Cu(GM)[12] and Cu(gly-L-ala).[13]

The coordination of the peptide oxygen O(1) is less common. Four Cu(II) and Zn(II) complexes have been reported: Zn(glycylglycine)$_2$·2H$_2$O,[33] Zn(glycylglycylglycine)(SO$_4$)$_{1/2}$·4H$_2$O,[36] Cu(glycylglycylglycine)Cl·1.5H$_2$O,[37] and Cu$_2$(glycyl-L-leucyl-L-tyrosine)$_2$·8H$_2$O.[38] In these cases, however, the peptide groups bind to the metal ion only through the oxygen atom. A nonchelating mode, as in the present work, for the peptide oxygen has been reported for Na(L-cysteinylglycine)I[34] and Ca(glycylglycylglycine)(H$_2$O)$_2$·Cl$_2$·H$_2$O.[35]

Apart from the previously mentioned compounds which exhibit some similarities to Cu(MG), only two recent complexes, Cu(GM)[12] and Cu(Gly-L-Ala),[13] show exactly the same kind of coordination. The observed distances and angles in the chelate rings are of the same magnitude. However, two significant differences between Cu(MG) and the two other compounds may be mentioned. The first one is the shortening of the N(2)–C(2) bond in Cu(MG) associated with an asymmetrical coordination of N(2) (Table VI).

The second one concerns the significant shortening of the S–C bonds although in Cu(GM) and Cu(MG) there is no direct interaction between the thioether side chain and the metal ion (Table VII).

The Cu–O(1)–C(2) angle has a different value from that found in the above mentioned complexes, with the exception of the Ca complex[35] (Ca–O(1)–C(1) = 144.1° and Ca–O(2)–C(2) = 148.9°). The unusually high value of the Cu–O–C angle in our L-methionylglycine complex compared with Cu(GM) (139.6°) and Cu(gly-L-ala) (126.8°) is very likely due to the steric requirements of the bidentate peptide group.

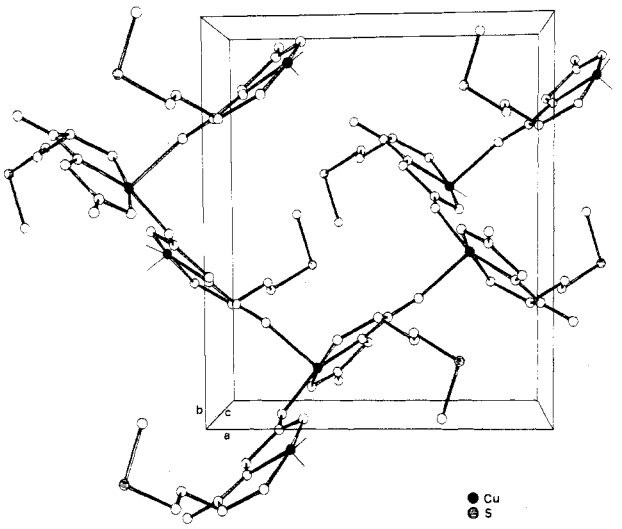

Figure 4. A view of the unit cell packing.

Shortest intermolecular distances within the cell unit are reported in Table VIII. The crystal packing is illustrated in the view of Figure 4.

IR and ^{1}H NMR Spectra Results. The assignments of the free dipeptides L-methionylglycine and glycyl-L-tyrosine and of their Cu complexes by infrared and Raman spectra are based on those of Condrate and Nakamoto,[39] Kieft and Nakamoto,[40] Podlaha and Podlahova,[41] and Herlinger et al.[43]

Only absorptions assigned to the most significant ligand functions of the peptides are included in Table IX. Both glycyl-L-tyrosine and L-methionylglycine show only the absorptions corresponding to the zwitterionic structure.

The extensive hydrogen bonding of the peptides makes it difficult to rationalize frequency shifts upon metal coordination, because of the accompanying changes in the extent of the hydrogen bonding. It is interesting to note, however, the disappearance of the $\nu_{as}(NH_3^+)$ band associated with the zwitterionic structure, coupled with the appearance of two absorptions in the 3100–3300-cm^{-1} region assigned to the N–H stretching mode. These changes are in agreement with the fact that in both complexes the terminal NH_2 group of the peptides occupies one of the coordination sites of the Cu(II) ion. The band due to the asymmetric mode of the carboxylate appears at a lower frequency in both complexes. On the contrary the $\nu_s(COO^-)$ is shifted from 1384 to 1405 cm^{-1} in [Cu(GT)(H$_2$O)$_2$]·2H$_2$O, while it disappears for Cu(MG). These results indicate that the carboxyl group is coordinated[33] in both cases. No significant difference is visible, however, between the two spectra, as could be expected for the two different types of coordination, monodentate (gly-L-tyr) and

Table IX. Infrared and Raman Spectral Data (cm^{-1})

				$\nu(COO^-)$				
	ν(N-H)	$\nu_{as}(NH_3^+)$	ν(amide I)	asym	sym	ν(C-S)	ν(Cu-N)	ν(Cu-O)
GT	3336 s	3030 m	1660 s	1603 s	1384 m			
[Cu(GT)(H$_2$O)$_2$]·2H$_2$O		3242 m 3160 m	1600 s	1584 s	1405 m		410 m 405 m	321 m
MG	3350 m	3080 m	1660 s	1617 s	1380 s	713 m, 710 m 697 m, 696 m		
Cu(MG)		3342 m 3292 m	1615 s	1585 s		723 m, 704 m	450 m 440 m	365 m

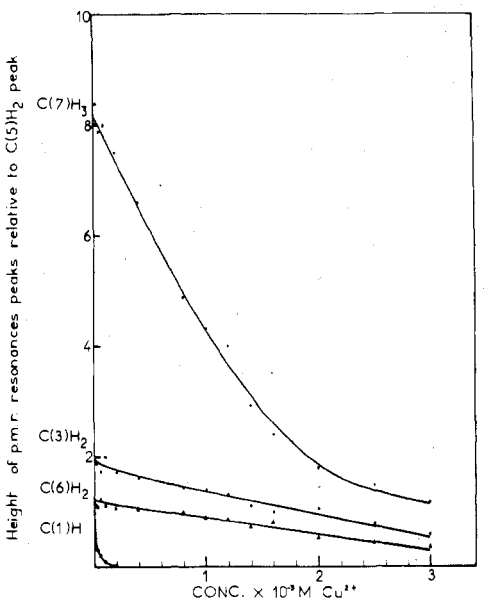

Figure 5. Line broadening of ^1H NMR spectra of L-methionylglycine (0.1 M) in D_2O, pD 4.9, with increasing amounts of $CuCl_2$.

bridging two Cu ions through both oxygen atoms (met-gly). This lack of different spectroscopic behavior could be explained by the low symmetry of the free ion $-COO^-$.

The amide I absorption appears at 1660 cm^{-1} in the free dipeptides and decreases to 1600 cm^{-1} in $[Cu(GT)(H_2O)_2]\cdot 2H_2O$. As shown by the X-ray data, and in agreement with the observations of Martell and Kim,[44] this indicates that the peptide group is coordinated to the metal only through its deprotonated nitrogen. On the other hand, the amide I band of Cu(MG) appears at 1615 cm^{-1} and its intermediate between the 1600–1605-cm^{-1} range, typical of a peptide N bonding, and the 1620–1625-cm^{-1} range, typical of a peptide O bonding.[44] Thus, in the solid state, there is only indirect IR evidence that the peptide group in L-methionylglycine is bound to the Cu atoms through both its deprotonated nitrogen and ketone oxygen.

The infrared C–S stretching modes of L-methionylglycine give, upon coordination, only one absorption band at a high frequency while the two Raman visible peaks coalesce and yield a single band at an intermediate frequency. These results are not indicative, however, of a thioether coordination to the metal, as shown by the structural examination.

The far-infrared spectra of the complexes contain several bands of medium intensity, assigned to the copper–ligand stretching frequencies. Thus, in agreement with Condrate and Nakamoto[39] and Herlinger et al.,[42] we have attributed the peaks in the 450–400-cm^{-1} range to the ν(Cu–N) modes. The Cu–O stretching frequencies appear at 321 and 365 cm^{-1}. The latter is a somewhat higher value than generally reported because of coordination of the carboxyl group to the two metals.

The ^1H NMR line broadening induced by the Cu^{2+} ion was used to gain additional information on the dipeptide mode of binding. We report in Figure 5 the observed flattening of the L-methyl peaks, relative to the signal given by the C(5) protons in the presence of increasing amounts of $CuCl_2$. The most significant result is the disappearance of the C(1)H peak at a lower metal concentration (0.2 mmol) than that required for the other peaks. This behavior, indicates that the terminal amino group, proximal to the C(1) atom, is the first bind to the metal ion.[20,45–48] The methyl protons of the thioether group are also quite strongly influenced by the presence of Cu^{2+} but there is no definite indication that an interaction of the thioether sulfur with the metal atom is actually occurring.

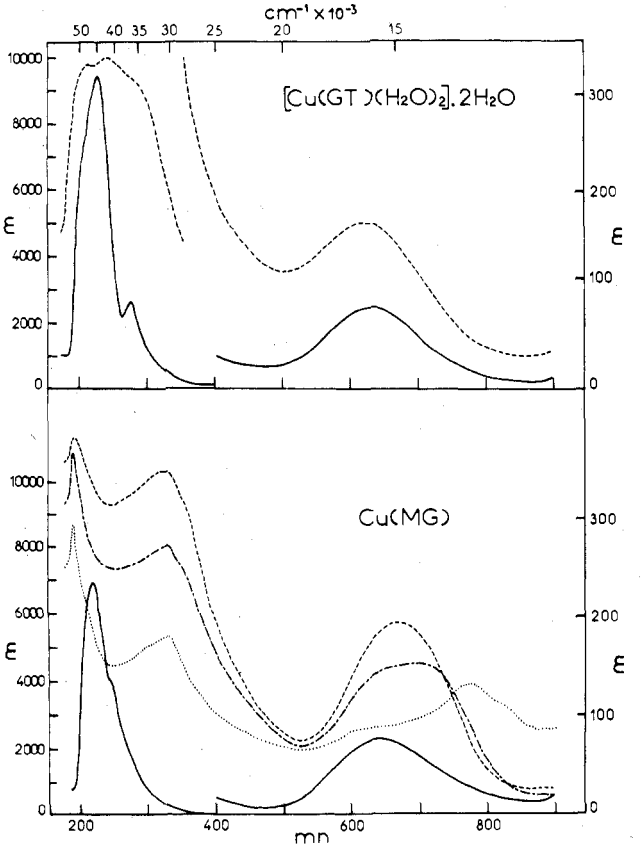

Figure 6. Absorption spectra of $[Cu(GT)(H_2O)_2]\cdot 2H_2O$ and Cu(MG): water solution spectra (–); solid-state spectra in KBr (- - -); Cu(MG) solid-state spectra in KBr (– · –) 2 days and (···) 4 days after the preparation of the pellet.

Electronic and Magnetic Properties. The ultraviolet and visible spectra of the copper complexes are presented in Figure 6. The absorption spectra of $[Cu(GT)(H_2O)_2]\cdot 2H_2O$ and Cu(MG) in water at pH $\simeq$6.5 exhibit a broad maximum at 630 nm (ϵ 89) and 640 nm (ϵ 76), respectively. The d–d band position is determined by the ligand field contributions from the four donor atoms which, with Cu, define the square plane. Our results are indicative of mixed O and N donor groups,[49] in agreement with literature data for 1:1 copper–dipeptide neutral complexes.[45,50–52]

Charge-transfer bands (in aqueous solution) are visible at 275 (ϵ 2550) and 225 nm (ϵ 9200) for the gly-L-tyr complex and at 240 (sh) (ϵ 4150) and 220 nm (ϵ 6900) for the L-metgly complex. The lowest energy absorption in the free glycyl-L-tyrosine occurs at 276 nm (ϵ 1360) and is due to charge transfer within the phenyl ring. The increase in intensity of this band after complexation is caused by its superposition with a $CO_2 \rightarrow Cu$ charge-transfer band absorption.[53] The same band appears at a shorter wavelength (240 nm) in Cu(MG). Electronic spectra of Cu(II) complexes of ethylamine and various amino acids and of the bis Cu(II) complexes of ethylenediamine exhibit σ(N) $\rightarrow$ Cu(II) LMCT at $\sim$230 nm[53,54] which are not perturbed by apical ligand–Cu interactions. By analogy, we assign the absorption at 220–225 nm to a σ(N) $\rightarrow$ Cu(II) LMCT.

In order to assess whether the complexes will adopt a comparable structure in the solid state and in solution, solid-state spectra were also recorded. The absorption spectrum of $[Cu(GT)(H_2O)_2]\cdot 2H_2O$ as a KBr pellet exhibits a broad band at 622 nm and an ultraviolet absorption at 237 nm with two shoulders at 220 and 275 nm. These bands are respectively assigned to the ligand field absorption of the CuN_2O_3 ligand set (622) and to the σ(N) $\rightarrow$ Cu (220) and $CO_2 \rightarrow$ Cu (275)

Table X. Magnetic and ESR Data

	μ_{eff}, μ_B	g_x	g_y	g_z	g_0[a]	$10^4 A_N$, cm^{-1}
$[Cu(GT)(H_2O)_2]\cdot 2H_2O$	1.92	2.186	2.109	2.059	2.118	12
Cu(MG)	1.86	2.166	2.151	2.065	2.127	

[a] $g_0^2 = {}^1/_3(g_x^2 + g_y^2 + g_z^2)$.

LMCT. Since no significant electronic spectral differences in intensity and shape are visible between the solid-state and the solution spectra, it can be assumed that the five-coordinate square-pyramidal geometry of the glycyl-L-tyrosine copper complex found in the crystal persists in solution.

Significant differences are observed, however, when comparing the solution and the solid-state electronic spectra of Cu(MG). Thus, a new band is visible at 325 nm, which disappears in aqueous solution. A similar absorption has been observed with other copper carboxylic acid dimers, where the COO^- group is bridging between two metal atoms.[55,56] Yamada et al.[57] suggested that the band is a diagnostic property of the copper–copper linkage. Dubicki and Martin,[58] on the other hand, proposed this band to be characteristic of the carboxylate bridging π system, on the basis of a Hückel molecular orbital calculation. The Cu(MG) crystal structure analysis shows the carboxyl group binding to two metal atoms, with a syn–anti disposition of the metal–oxygen bonds which excludes any Cu–Cu interaction. The 325-nm absorption can therefore be attributed to the bridging π system which is delocalized over the COO group and the Cu atoms.

The ligand field absorption appears at 672 nm in the solid state. Its shift to a higher energy (640 nm) upon dissolution in water and the simultaneous disappearance of the band at 325 nm are indicative of a cleavage of the $Cu–CO_2–Cu$ bridge and of its partial replacement by a water molecule in the metal coordination sphere. Indeed, in the spectrochemical series, H_2O produces a higher ligand field than does COO^-[59] and causes a shift of the d–d band to a shorter wavelength. According to Freeman,[11] the peptide oxygen–copper band persists in solution even if, as in the case of Cu(MG), it is in apical position. Moreover, the replacement of the peptide oxygen by H_2O would have little influence on the d–d band position, since the ligand fields produced by either of these two groups are similar. Further evidence of the replacement of one of the carboxylate oxygens by H_2O, when the crystal is dissolved in water, is given by the fact that the spectrum of Cu(MG) in solution is almost identical with those of $[Cu(GT)(H_2O)_2]\cdot H_2O$. It is probable therefore that (L-methionylglycinato)copper(II) will adopt a comparable coordination structure in solution, with a water molecule in equatorial position.

The solid-state electronic spectrum of Cu(MG) was observed to change in time (see Figure 6). The d–d absorption band is shifted to a lower energy and splits (λ_{max} 774 nm after 4 days), while the absorptivity at 325 nm has decreased ca. 65%. Simultaneously, a decrease in intensity of the infrared ν(amide I) and $\nu_{as}(COO^-)$ bands has occurred. These results suggest that a reaction between the complex and the KBr is taking place within the KBr pellet. Indeed, the replacement of one of the carboxylate oxygens (indicated by the progressive weakening of the absorption at 325 nm) by the bromide in the copper coordination sphere is known to produce a similar shift of the d–d absorption to the lower energies.[45]

The effective magnetic moments (see Table X) lie in the 1.8–2.0-μ_B range and are typical of "magnetically dilute" complexes[60] where the individual copper(II) ions are separated from each other (no antiferromagnetic interactions can thus occur). The single-crystal ESR parameters at 300 K are in good agreement with those reported by Boas et al.[61] and Falk et al.[62] for analogous neutral species of copper(II) dipeptide complexes. Additional superhyperfine splitting is visible in the aqueous solution (10% methanol) spectrum of $[Cu(GT)(H_2O)_2]\cdot 2H_2O$. This is caused by the unpaired electrons of the copper atom interacting with the glycyl-L-tyrosine nitrogen nuclei. The nitrogen hyperfine coupling constant ($A_N = 12 \times 10^{-4}$ cm^{-1}) is consistent with literature data for copper(II) amino acid[63] and dipeptide[64] complexes.

Registry No. $[Cu(GT)(H_2O)_2]\cdot 2H_2O$, 64421-84-7; Cu(MG), 69687-59-8.

References and Notes

(1) G. I. Eichorn, Ed., "Inorganic Biochemistry", Elsevier, Amsterdam, 1973, and references therein.
(2) H. Sigel, Ed., "Metal Ions in Biological Systems", Marcel Dekker, New York, 1974, and references therein.
(3) S. Lindskog, *Struct. Bonding (Berlin)*, **8**, 153 (1970); M. Llinas, *ibid.*, **17**, 135 (1974); A. S. Mildvan and C. M. Grisham, *ibid.*, **20**, 1 (1975); J. A. Fee, *ibid.*, **23**, 1 (1975); M. F. Dunn, *ibid.*, **23**, 61 (1975).
(4) M. L. Bender in "Mechanisms of Homogeneous Catalysis from Protons to Proteins", Wiley-Interscience, New York, 1971.
(5) R. W. Hay and P. J. Morris in "Metal Ions in Biological Systems", Vol. 5, H. Sigel, Ed., Marcel Dekker, New York, 1976, pp 128–243.
(6) R. C. Rosenberg, C. A. Root, P. K. Berstein, and H. B. Gray, *J. Am. Chem. Soc.*, **97**, 2092 (1975).
(7) J. E. Coleman and B. L. Vallee, *J. Biol. Chem.*, **236**, 2244 (1961).
(8) J. E. Coleman, P. Pulido, and B. L. Vallee, *Biochemistry*, **5**, 2019 (1966).
(9) M. Schneider, J. Suh, and E. T. Kaiser, *J. Chem. Soc., Chem. Commun.*, 106 (1976).
(10) M. L. Ludwig and W. N. Lipscomb in "Inorganic Biochemistry", G. L. Eichorn, Ed., Elsevier, Amsterdam, 1973, pp 438–487.
(11) H. C. Freeman in "Inorganic Biochemistry", G. L. Eichorn, Ed., Elsevier, Amsterdam, 1973, pp 121–166.
(12) C. A. Bear and H. C. Freeman, *Acta Crystallogr., Sect. B*, **32**, 2534 (1976).
(13) H. C. Freeman, M. J. Healy, and M. L. Scudder, *J. Biol. Chem.*, **252**, 8840 (1977).
(14) M. V. Veidis and G. J. Palenik, *Chem. Commun.*, 1277 (1969).
(15) P. R. Milne, J. R. E. Wells, and R. P. Ambler, *Biochem. J.*, **143**, 691 (1974).
(16) R. Nakon, E. M. Beadle, Jr., and R. J. Angelici, *J. Am. Chem. Soc.*, **96**, 719 (1974).
(17) T. E. Jones, D. B. Rorabacher, and L. A. Ochrymowycz, *J. Am. Chem. Soc.*, **97**, 7485 (1975).
(18) A. R. Amundsen, J. Whelan, and B. Bosnich, *J. Am. Chem. Soc.*, **99**, 6730 (1977).
(19) H. Sigel, C. F. Naumann, B. Prijs, D. B. McCormick, and M. C. Falk, *Inorg. Chem.*, **16**, 790 (1977).
(20) J. Dehand, J. Jordanov, and F. Keck, *Inorg. Chim. Acta*, **21**, L13 (1977).
(21) A. Mosset and J. J. Bonnet, *Acta Crystallogr., Sect. B*, **33**, 2807 (1977).
(22) A. Mosset, J. J. Bonnet, and J. Galy, *Acta Crystallogr., Sect. B*, **33**, 2639 (1977).
(23) W. R. Busing, K. O. Martin, and H. A. Levy, "ORFEE", Report ORNL-TM.306, Oak Ridge National Laboratory, Oak Ridge, Tenn., 1964.
(24) C. K. Johnson, "ORTEP", Report ORNL-3794, Oak Ridge National Laboratory, Oak Ridge, Tenn.
(25) D. T. Cromer and J. T. Waber, "International Tables for X-Ray Crystallography", Vol. 4, Kynoch Press, Birmingham, England, 1974, Table 2.2.A.
(26) W. H. Zachariasen, *Acta Crystallogr., Sect. A*, **24**, 212 (1968).
(27) E. L. Muetterties and L. J. Guggenberger, *J. Am. Chem. Soc.*, **96**, 1748 (1974).
(28) J. T. Edsall, P. J. Flory, J. C. Kendrew, A. M. Liquori, G. Nemethy, G. M. Ramachandran, and H. A. Scheraga, *Biopolymers*, **4**, 121 (1966).
(29) J. D. Bell, H. C. Freeman, A. M. Wood, R. Driver, and W. R. Walker, *Chem. Commun.*, 1441 (1969).
(30) M. B. Hursthouse, S. A. A. Jayaweera, G. H. W. Milburn, and A. Quick, *Chem. Commun.*, 207 (1971).
(31) D. Van Der Helm, S. E. Ealick, and J. E. Burks, *Acta Crystallogr., Sect. B*, **31**, 1013 (1975).
(32) V. Amirthalingam and K. V. Muralidharan, *Acta Crystallogr., Sect. B*, **32**, 3153 (1976).
(33) H. C. Freeman, *Adv. Protein Chem.*, **22**, 257 (1967).
(34) H. B. Dyer, *Acta Crystallogr.*, **4**, 42 (1951).
(35) D. Van Der Helm and T. V. Willoughby, *Acta Crystallogr., Sect. B*, **25**, 2317 (1969).
(36) D. Van Der Helm and H. B. Nicholas, *Acta Crystallogr., Sect. B*, **26**, 1858 (1970).

(37) H. C. Freeman, G. Robinson, and J. C. Schoone, *Acta Crystallogr.*, **17**, 719 (1964).
(38) W. A. Franks and D. Van Der Helm, *Acta Crystallogr., Sect. B*, **27**, 1299 (1970).
(39) R. A. Condrate and K. Nakamoto, *J. Chem. Phys.*, **42**, 2590 (1965).
(40) J. A. Kieft and K. Nakamoto, *Inorg. Chim. Acta*, **2**, 225 (1968).
(41) J. Podlaha and J. Podlahova, *Inorg. Chim. Acta*, **5**, 413 (1971).
(42) A. W. Herlinger, S. L. Wenhold, and T. V. Long, II, *J. Am. Chem. Soc.*, **92**, 6474 (1970).
(43) F. R. Dollish, W. G. Fateley, and F. F. Bentley, "Characteristic Raman Frequencies of Organic Compounds", Wiley-Interscience, New York, 1974.
(44) A. E. Martell and M. K. Kim, *J. Coord. Chem.*, **4**, 9 (1974).
(45) M. K. Kim and A. E. Martell, *Biochemistry*, **3**, 1169 (1964).
(46) R. Mathur and R. B. Martin, *J. Phys. Chem.*, **69**, 668 (1965).
(47) M. K. Kim and A. E. Martell, *J. Am. Chem. Soc.*, **91**, 872 (1969).
(48) D. B. McCormick, R. Giesser, and H. Sigel in "Metal Ions in Biological Systems", Vol. 1, Marcel Dekker, New York, 1974, pp 213–247.
(49) R. Zand and G. Palmer, *Biochemistry*, **6**, 999 (1967).
(50) A. P Borisova, I. V. Igonina, N. F. Stepanov, and D. I. Ismailov, *Russ. J. Inorg. Chem. (Engl. Transl.)*, **20**, 1048 (1975).
(51) E. J. Billo, *Inorg. Nucl. Chem. Lett.*, **10**, 613 (1974).
(52) M. C. Lim, E. Sinn, and R. B. Martin, *Inorg. Chem.*, **15**, 807 (1976).
(53) V. C. Miskowski, J. A. Thich, R. Solomon, and H. J. Schugar, *J. Am. Chem. Soc.*, **98**, 8344 (1976).
(54) E. W. Wilson, Jr., M. H. Kasperian, and R. B. Martin, *J. Am. Chem. Soc.*, **92**, 18, 5365 (1970).
(55) W. E. Hatfield and R. Whyman in "Transition Metal Chemistry", Vol. 5, Marcel Dekker, New York, 1969, p 105.
(56) A. E. Hansen and C. J. Ballhausen, *J. Chem. Soc. A*, **61**, 631 (1965).
(57) S. Yamada, H. Nakamura, and R. Tsuchida, *Bull. Chem. Soc. Jpn.*, **30**, 953 (1957); **31**, 303 (1958).
(58) L. Dubicki and R. L. Martin, *Inorg. Chem.*, **5**, 2203 (1966).
(59) D. Sutton, Ed., "Electronic Spectra of Transition Metal Complexes", McGraw-Hill, London, 1968, p 162.
(60) B. J. Hathaway and D. E. Billing, *Coord. Chem. Rev.*, **5**, 143 (1970).
(61) J. B. Boas, J. R. Pilbrow, C. R. Hartzell, and T. D. Smith, *J. Chem. Soc. A*, 572 (1969).
(62) K. E. Falk, H. C. Freeman, T. Jansson, B. G. Malmstrom, and T. Vanngard, *J. Am. Chem. Soc.*, **89**, 6071 (1967).
(63) R. H. Fish, J. J. Windle, W. Gaffield, and J. R. Scherer, *Inorg. Chem.*, **12**, 855 (1973).
(64) H. Kozlowski and B. Jezowska-Trzebiatowska, *J. Inorg. Nucl. Chem.*, **39**, 1275 (1977).

Contribution from the U.E.R. de Chimie and Ecole Nationale Superieure de Chimie de Lille, Université de Lille I, 59650 Villeneuve d'Ascq, France

Influence of π Back-Bonding on the Reactivity of the Nitrosyl Group. Nitrosation of Activated Methylene Compounds via Nitrosyl–Ruthenium Complexes

CLAUDE BREMARD,*[1a] GUY NOWOGROCKI,[1b] and STEPHANE SUEUR[1b]

Received September 22, 1978

In an effort to probe the mechanism of nitrosation of activated methylene compounds through nitrosyl complexes, the reactions of a series of β-diketones with neutral nitrosyl–ruthenium complexes $Ru(AB)_2NOX$ have been investigated (AB is the monoanion of 2,4,6-trioxo-5-oximinopyrimidine or 1,3-dimethyl-2,4,6-trioxo-5-oximinopyrimidine; X = Cl, Br, OH, NO_2). The rate of the nitrosation reaction is strongly dependent on the acidity of the activated methylenes, the nature of the solvent, and the coordination environment of the nitrosyl group. The latter behavior is assessed in terms of the nitrosyl π^* acceptor orbital.

Nitrosyl ligand, as well as other ligands which contain metal–nitrogen multiple bonds, is of current interest. Structural[2-4] and synthetic[5] studies have shown the reactions of these ligands to be extremely varied. Whereas some nitrosyl complexes react as electrophiles,[6-10] others react as nucleophiles.[11-17] Because of the important role played by back-donation on the reactivity of coordinated nitrosyl, the development of a means to obtain quantitative information concerning the nature of metal-to-ligand π bonding has been of great interest in recent years.[13,14] N 1s bonding energy and NO stretching frequencies (or the derived force constant) of transition-metal nitrosyls have commonly been used to measure the degree of back-bonding.[4] There is a good correlation between ν(NO) frequencies and the electronic occupation of the π^* orbital of nitrosyl.[15] The nitrosyl complexes with high values of ν(NO) react with nucleophiles and the reactivity can be attributed to degree of NO^+ character.[8,10,16]

Earlier,[17,18] we reported the preparation and stereochemistry of new neutral ruthenium–mononitrosyl complexes *cis*-$Ru(AB)_2NOX$, where AB represents the unsymmetrical bidentate ligands 1,3-dihydrogenoviolurate, denoted H_2vi^-, or 1,3-dimethylviolurate, $dmvi^-$, and X represents Cl, Br, NO_2, OH, or monodentate AB.

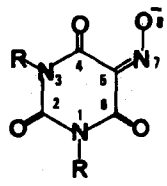

R = R′ = H, 1,3-dihydrogenoviolurate, H_2vi
R = R′ = CH_3, 1,3-dimethylviolurate, dmvi

All these complexes possess nitrosyl groups with high ν(NO) stretching frequencies. The unusual reactivity of the nitrosyl complexes can be attributed to a considerable degree of NO^+ character in the formal (d^6) Ru(II)–NO^+ linkage caused by the relatively high formal oxidation state of the metal and the competitive back-bonding with the AB ligands. The effects of metal-to-ligand AB π back-bonding in $Ru(AB)_2NOX$ have been investigated by changes in ^1H NMR chemical shifts.[18] Moreover, in the case of $Ru(H_2vi)_2NOX$,[19] the capacity of the nitrosyl ligand to act as an electron pump[20,21] was demonstrated by a very important increasing of the acidity of the deprotonation sites in the coordinated heterocycle. The effects of H_2vi^-, Hvi^{2-}, and vi^{3-} as auxiliary ligands on the reactivity of the NO group of *cis*-$[Ru(H_pvi)_2NOCl]^{2p-4}$ ($2p$ = 0–4) with an activated methylene group to form N–C bonds attracted us to the present study. The formation of N–C bonds via intermediate ruthenium–nitrosyl complexes has been described in some instances,[9,22,23] and nitrosoarenes[24] and nitrosoalkanes[25] have proved to be interesting ligands of iron(II) porphyrins and hemoproteins. The present work is part of an effort meant to explore the mechanism of nitrosation of organic substrates via nitrosyl complexes.

Experimental Section

Materials. Barbituric acid (Merck), dimethylbarbituric acid (Fluka), dimedon, acetylacetone, ethyl acetoacetate, and diethyl malonate (Prolabo) were used without further purification.

Physical Measurements. UV–vis spectra were run on a Jobin and Yvon DUOSPAC 230 spectrophotometer using jacketed quartz cells. Infrared spectra were obtained on a Beckman IR20 AX with KBr plates and Nujol mulls. ^1H NMR spectra were taken on a Perkin-Elmer R 24 B. The potentiometric data were collected on a Radiometer PM 52 instrument employing a glass electrode (solution)|KCl (saturated solution) calomel electrode.

0020-1669/79/1318-1549$01.00/0